

Research Article

An Automatic Emergency Braking Model considering Driver's Intention Recognition of the Front Vehicle

Wei Yang ¹, Jiajun Liu ¹, Kaixia Zhou ¹, Zhiwei Zhang ¹ and Xiaolei Qu ^{2,3}

¹School of Automobile, Chang'an University, Xi'an 710064, China

²School of Instrumentation and Optoelectronic Engineering, Beihang University, Beijing 100083, China

³Beijing Advanced Innovation Center for Big Data-Based Precision Medicine, Beihang University, Beijing 100083, China

Correspondence should be addressed to Wei Yang; yw@chd.edu.cn

Received 10 February 2020; Revised 13 October 2020; Accepted 21 November 2020; Published 8 December 2020

Academic Editor: Eleonora Papadimitriou

Copyright © 2020 Wei Yang et al. This is an open access article distributed under the Creative Commons Attribution License, which permits unrestricted use, distribution, and reproduction in any medium, provided the original work is properly cited.

Driver's intention of the front vehicle plays an important role in the automatic emergency braking (AEB) system. If the front vehicle brakes suddenly, there is potential collision risk for following vehicle. Therefore, we propose a driver's intention recognition model for the front vehicle, which is based on the backpropagation (BP) neural network and hidden Markov model (HMM). The brake pedal, accelerator pedal, and vehicle speed data are used as the input of the proposed BP-HMM model to recognize the driver's intention, which includes uniform driving, normal braking, and emergency braking. According to the recognized driver's intention transmitted by Internet of vehicles, an AEB model for the following vehicle is proposed, which can dynamically change the critical braking distance under different driving conditions to avoid rear-end collision. In order to verify the performance of the proposed models, we conducted driver's intention recognition and AEB simulation tests in the co-simulation environment of Simulink and PreScan. The simulation test results show that the average recognition accuracy of the proposed BP-HMM model was 98%, which was better than that of the BP and HMM models. In the Car to Car Rear moving (CCRm) and Car to Car Rear braking (CCRb) tests, the minimum relative distance between the following vehicle and the front vehicle was within the range of 1.5 m–2.7 m and 2.63 m–5.28 m, respectively. The proposed AEB model has better collision avoidance performance than the traditional AEB model and can adapt to individual drivers.

1. Introduction

Rear-end collisions are the most common traffic accidents, with more than 90% due to drivers' inattention or nervousness [1]. The National Transportation Safety Board (NTSB) points out that 80% of rear-end collisions can be avoided by using advanced collision avoidance systems [2].

The automatic emergency braking system (AEB) is a typical advanced collision avoidance system, which uses onboard sensors to detect collision risk and automatically brakes when necessary to avoid collision. According to the research report [3], when the vehicle speed is less than 50 km/h, vehicles using the AEB system can reduce the rear-end accidents by 38%. Therefore, it is of great significance to study the AEB system.

It is the keys for the AEB system to judge the dangerous degree and establish the collision avoidance model. Many

studies use safety braking distance [4–6] or time to collision (TTC) [7–9] for risk measurement. There are also many improvements based on these models. Katare and El-Sharkawy [10] proposed a collision warning model using the neural network based on supervised learning to provide early warning of possible collisions. Chen et al. [11] proposed a new algorithm that considered both time collision and safety braking distance. Kaempchen et al. [12] proposed a method to calculate the AEB emergency braking trigger time, which considered all possible trajectories and dimensions of the target and host vehicle. Pei et al. [13] proposed the concept of collision avoidance time margin on the basis of known workshop motion information, and a hierarchical alarm/collision avoidance algorithm applicable to different drivers' collision avoidance characteristics was designed. In addition, many scholars also consider the impact of pavement conditions on AEB performance. Han

et al. [14] proposed an AEB braking strategy that considered the impact of different road friction on the TTC braking threshold. Kim et al. [15] proposed an algorithm for estimating the maximum tire-road friction coefficient based on interacting multiple models and applied it to the AEB system. Hwang and Choi [16] used early-warning braking to estimate the maximum friction coefficient of tire pavement in real time to obtain road adhesion state and predicted rear-end collision risk adaptively based on friction information. Kim et al. [17] proposed an AEB control algorithm that can compensate for the impact of slope and road friction. Most of the parameters of the above research model cannot be adjusted online and cannot adapt well to the driver's behavior under different traffic conditions.

Recently, to improve the robustness of the system, the research on driver behavior is paid more attention. Li et al. [18] studied the visual scanning behavior of Chinese drivers at signalized and unsignalized intersections. Their other study [19] found that traffic congestion has a negative impact on driver behavior on the road after congestion, which provides a reference for the development of subsequent assistance systems. For the anticollision model, many research studies begin to consider the adaptive model of driver characteristics. Xiong et al. [20] developed an online risk-level classification algorithm based on several safety indexes such as TTC, time headway, and relative distance under emergency braking. Duan et al. [21] extracted three main vehicle-bicycle conflict scenarios from naturalistic driving data, analyzed the impact of conflict types on Chinese drivers' braking behavior, and proposed a design method of adaptive Bicyclist-AEB based on driver braking characteristics. Wada et al. [22] expressed the deceleration mode of the professional drivers' braking at the last second with a perceived risk index and applied it to the AEB system. Wang et al. [23] proposed a forward collision warning algorithm that can adjust the warning threshold in real time according to the driver's behavior change. Bella and Russo [24] analyzed the driver's behavior, determined an effective driver assistance system which can be readily accepted by the driver, and then proposed a new collision warning algorithm based on the driver's risk perception. Lee et al. [25] used an artificial neural network learning algorithm to establish a driver behavior model. The collision risk was determined according to the driving characteristics of the driver. Wang et al. [26] used a driving simulator to simulate brake-only noncollision events and then used the driver's braking behavior to simulate the driver's expected response decelerations. There are also many studies that take into account the driving behavior or intentions of other vehicles. Yuan et al. [27] proposed a method to predict the lane change maneuver intention of vehicles in front by using the hidden Markov model. Geng et al. [28] used HMM to learn the continuous characteristics of driving behavior and predicted the behavior of the target vehicle by combining the posterior probability and prior probability. Hu et al. [29] used semantics to define vehicle behavior and a probabilistic framework based on deep neural networks to estimate the driver's intention, final position, and corresponding time information of surrounding vehicles. Jo et al. [30] proposed a

unified vehicle tracking and behavior reasoning algorithm, which can simultaneously estimate the dynamics of surrounding vehicles and the intentions of drivers. These studies mainly use sensors to obtain the state that the vehicle has shown, they set off from data or models to adapt to the driver's behavior, and less consider the driving behavior of the surrounding vehicle drivers and their changing trends, although this may be as important as the driver's characteristics.

With the rapid development of the communication technology, the application of Internet of vehicles technology can make it easy to transmit data between vehicles [31–33]. Wu et al. [34] proposed a vehicle collision risk prediction method based on the Internet of vehicles, which can predict the vehicle collision risk by comprehensively considering the target vehicle's movement/position, driver behavior, and road information. Thomas et al. [35] proposed a collision avoidance system using Kalman filter and dedicated short-range communications (DSRCs) for intersection of straight and curved roads. Liu et al. [36] proposed a DSRC-based end of queue conflict early-warning system, which took into account not only the permeability of DSRC, but also the influence factors of traffic and communication. Tian et al. [37] proposed a method to use DSRC to predict vehicle movement behavior in collaborative vehicle environment. The above research is mainly applied to the early-warning system and only considers the behavior of the front vehicle without considering the time spent by the driver's behavior operation before the vehicle behavior changes, which may lead to the prediction lag. However, instead, these studies provide new ideas for AEB design.

In this article, we proposed an AEB model based on driver's intention recognition of the front vehicle. The model recognizes the driving intention of the front vehicle and transmits the information to the following vehicle through vehicle-to-vehicle communication technology. Compared with previous studies, this paper dynamically adds the driver's intention of the front vehicle into the AEB system of the following vehicle through vehicle-to-vehicle communication, so as to improve the performance of the collision avoidance system. The main contributions of this paper include the following: (1) a real-time driving intention recognition method with two-layer structure is proposed; (2) an AEB model is proposed based on safety distance and driving intention of the front vehicle; (3) the driving intention of the preceding vehicle is dynamically combined with the AEB system of the following vehicle.

The rest of the paper is organized as follows: Section 2 provides the detailed methodology of the proposed method. Section 3 provides the simulation experiment. Section 4 provides the experimental results. Section 5 is dedicated to the discussions. Section 6 summarizes the conclusions.

2. Methods

An AEB model was proposed, which was based on the driver's intention recognition of front vehicle via Internet of vehicles. This model was mainly composed of two parts: the driver's intention recognition model of the front vehicle and the AEB

model of the following vehicle. Figure 1 shows schematic diagram of system work. First, we established a driver's intention recognition model based on BP-HMM to recognize the uniform driving intention, normal braking intention, and emergency braking intention of the front vehicle's driver by the collected data of the brake pedal, accelerator pedal, and speed of the front vehicle. Second, the recognized driver's intention and other driving parameters of the front vehicle were transmitted to the following vehicle via Internet of vehicles. Finally, according to the driver's intention received, the proposed AEB model of the following vehicle changed the method for calculating the critical braking distance and adjusted AEB braking logic in real time.

2.1. Driver's Intention Recognition Model of the Front Vehicle. Driver's intention can be reflected by multiple driver's behaviors occurring simultaneously or continuously in a period. Considering the relationship between driver's behaviors and intentions, as well as the temporal characteristics of driver's behaviors, we first recognized the driver's behavior and then inferred the driver's intention from the recognized driver's behavior.

BP and HMM models are two kinds of models, which are commonly used to recognize driver behaviors and intentions. The BP model has simple structure and strong fault tolerance, but its training needs a large number of samples. The HMM model has a strong temporal modeling ability, which requires more prior knowledge support during training and is suitable for small samples. Therefore, we proposed a driver's intention recognition model based on BP and HMM, which makes full use of the classification ability of the BP neural network for big data and the mapping ability of HMM for time relation of small data [38].

Rear-end collisions mainly occur, while the speed of the front vehicle is lower than that of the following vehicle or the front vehicle is braking. Therefore, the proposed BP-HMM model mainly focuses on the recognition of the driver's intention during uniform speed, normal braking, and emergency braking.

Figure 2 shows the structure of the proposed BP-HMM model. The pedal displacement and pedal speed of the brake pedal and accelerator pedal were used as the BP model's input to recognize the driver's behavior of the front vehicle. We categorized common driver braking behaviors into six categories: slight pressing the brake pedal, normal pressing the brake pedal, rapid pressing the brake pedal, keeping the brake pedal in position, releasing the brake pedal, and no action of the brake pedal. Similarly, the driver's acceleration behaviors were also divided into six categories: normal pressing the accelerator pedal, rapid pressing the accelerator pedal, keeping the accelerator pedal in position, normal releasing the accelerator pedal, rapid releasing the accelerator pedal, and no action of the accelerator pedal. Then, the vehicle speeds were classified according to the range of vehicle speeds. The driver's behavior recognition results and classified vehicle speed were used as the HMM model's input to recognize the driver's intention of the front vehicle. The driver's intention HMMs were divided into uniform driving,

normal braking, and emergency braking. After the HMM model processing, the current driver's intention was recognized.

The BP neural network model was used as a classifier of the driver's behaviors, and its classification learning process consisted of forward propagation and backpropagation, as shown in Figure 3. A three-layer BP neural network can complete the mapping of arbitrary dimensions, and the complexity of the two types of BP networks to be constructed is the same, so both types of BP neural networks use the single hidden layer network. The structure consisted of single input layer, single hidden layer, and single output layer. In Figure 3, l represents the number of hidden layers and n_i, n_o represent the number of neurons in the input and output layers, respectively [39].

In the process of forward propagation, the pedal data $\mathbf{X} = (x_1, x_2, \dots, x_{n_i})^T$ were passed to the input layer, processed layer by layer through the hidden layer, and then transmitted to the output layer. The state of neurons in each layer only affects the state of neurons in the next layer, while the output layer finally outputs the classification results of the driver's behavior $\mathbf{Y} = (y_1, y_2, \dots, y_{n_o})^T$.

During the backpropagation, the result of the output layer is compared with the value $\mathbf{Z} = (z_1, z_2, \dots, z_{n_o})^T$ of the expected driver's behavior classification, and error δ will be returned according to the path of the original network connection. Then, the weight $\mathbf{w} = (\mathbf{w}^{(1)}, \mathbf{w}^{(2)}, \dots, \mathbf{w}^{(l+1)})^T$ and the bias $\mathbf{b} = (\mathbf{b}^{(1)}, \mathbf{b}^{(2)}, \dots, \mathbf{b}^{(l)})^T$ between the neurons will be modified. Therefore, the error can be gradually reduced until the error is limited to a predetermined range.

The activation function of the transfer process of this network uses the Sigmoid function, which is defined as

$$f(x) = \frac{1}{(1 + e^{-x})}. \quad (1)$$

Considering the requirements of training time and training accuracy, the adaptive gradient descent (AGD) algorithm was used as the backpropagation algorithm of the network.

The data collected from the brake pedal and the accelerator pedal were taken as input, and the classification results of the six braking or acceleration behaviors were taken as output. And the number of hidden layer neurons was calculated as follows:

$$n = \sqrt{n_o + n_i} + a, \quad (2)$$

where n_i is 20 and n_o is 6; a is an any constant between 1 and 10.

Then, different n was substituted for iterative training, and the number of neurons in the single hidden layer n of the two types of BP neural networks was finally confirmed to be 12 and 15, respectively.

The speed was divided into ten levels. The first nine levels correspond to the speeds of 0–10 km/h, 10–20 km/h, . . . , 80–90 km/h, and if the speed is greater than 90 km/h, it is the last level.

The recognized driver's behavior and classified vehicle speed were used as input of the HMM model to recognize

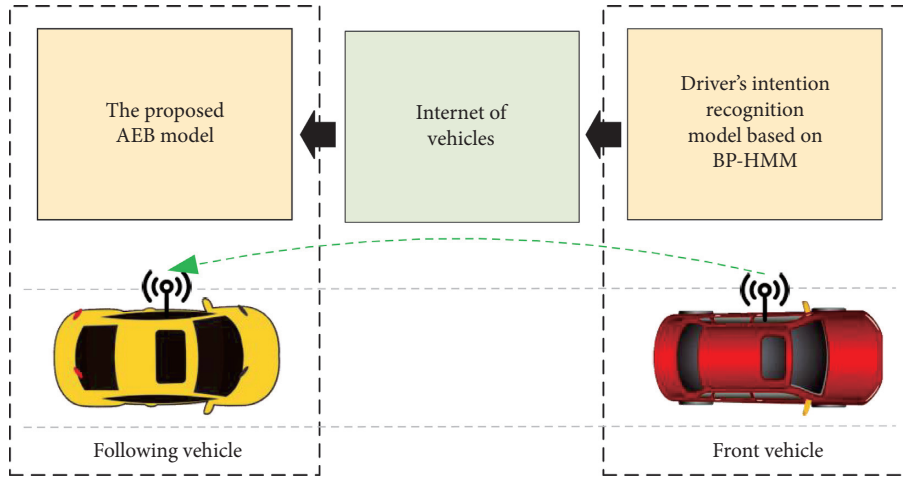


FIGURE 1: Schematic diagram of system work.

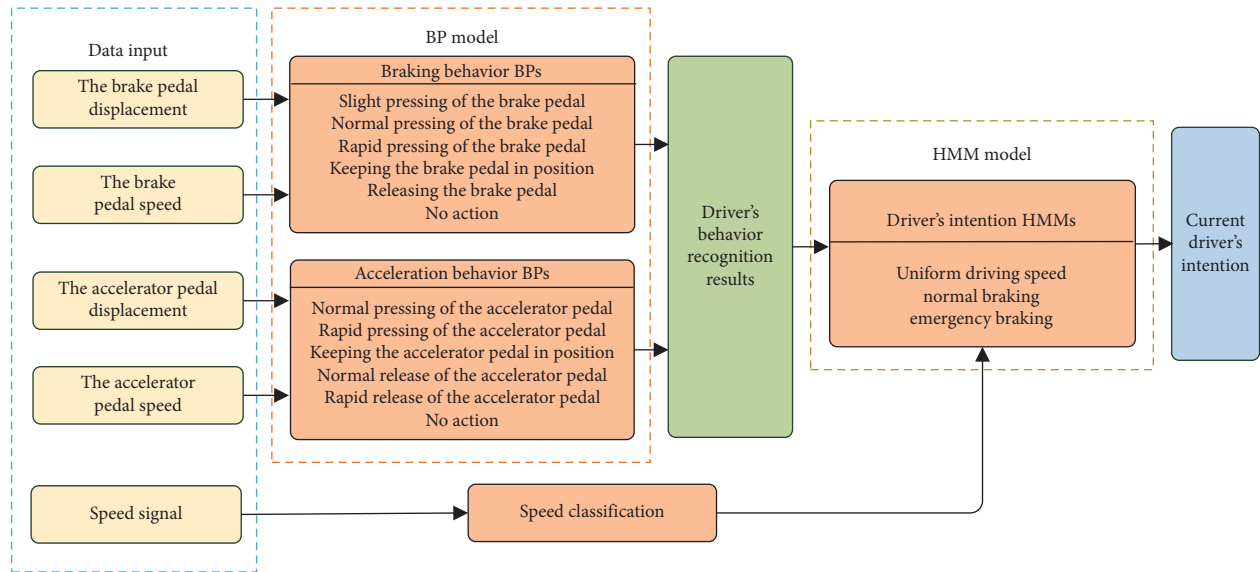


FIGURE 2: Structure of the proposed BP-HMM model.

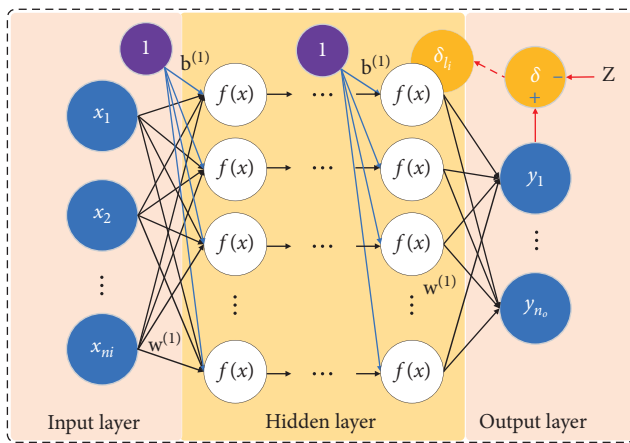


FIGURE 3: The structure of the BP neural network.

the driver's intention of the front vehicle, which can be defined as [40]

$$\mathbf{O}_t = \{\mathbf{x}(t), \mathbf{y}(t), \mathbf{z}(t)\}, \quad (3)$$

where $\mathbf{x}(t)$, $\mathbf{y}(t)$, and $\mathbf{z}(t)$ represent the classification results of the braking and acceleration behaviors and vehicle speeds, respectively.

Then, the driver's intention HMM can be expressed as follows:

$$\sigma = (\mathbf{A}, \mathbf{B}_x, \mathbf{B}_y, \mathbf{B}_z, \boldsymbol{\pi}), \quad (4)$$

where we used $\mathbf{Q} = \{q_1, q_2, q_3\}$ to indicate three driver's intentions; then, $\mathbf{A} = [\mathbf{a}_{ij}]_{3 \times 3}$ is the transition matrix of the driver's intentions from q_i to q_j . $\mathbf{B}_x = [\mathbf{b}_j^{(1)}(k)]_{3 \times 6}$, $\mathbf{B}_y = [\mathbf{b}_j^{(2)}(k)]_{3 \times 6}$, and $\mathbf{B}_z = [\mathbf{b}_j^{(3)}(k)]_{3 \times 10}$, respectively, represent the confusion matrix of three driver's intentions to each braking behavior, acceleration behavior, and

speed classification. π denotes the initial probability vector of the driver's intentions.

Since the input data of the HMM model is three-dimensional, the iterative formula of the forward and backward variables in the Baum–Welch algorithm needs to be modified as follows:

$$\begin{aligned}\alpha_{t+1}(j) &= \left[\sum_{i=1}^N \alpha_t(i) a_{ij} \right] \prod_{l=1}^L b_j(\mathbf{O}_{t+1}(l)), \\ \beta_t(i) &= \left[\sum_{j=1}^N a_{ij} \beta_{t+1}(j) \right] \prod_{l=1}^L b_j(\mathbf{O}_{t+1}(l)).\end{aligned}\quad (5)$$

The reevaluation formula of the Baum–Welch algorithm with multiple observation probability matrices was changed to

$$\bar{b}_j^{(l)}(k) = \frac{\text{count}(k^{(l)}|j)}{\text{count}(j)}, \quad (6)$$

where the forward variable $\alpha_{t+1}(j)$ denotes the probability when the partial observation sequence is $\mathbf{O}_1, \mathbf{O}_2, \dots, \mathbf{O}_{t+1}$ and the driver's intention is q_j at time $t+1$. The backward variable $\beta_t(i)$ denotes the probability that part of the observation sequence is $\mathbf{O}_{t+1}, \mathbf{O}_{t+2}, \dots, \mathbf{O}_T$ at the time t and the state is q_i . $\text{count}(k^{(l)}|j)$ represents the expectation of the observed value k in the l -th ($l = 1, 2, 3$) dimension of the observation sequence when the driver's intention is q_j . L is a constant, defined as 3.

The modified Baum–Welch algorithm was used to train the driver's intention HMMs, and then the HMM parameters of uniform speed driving, normal braking, and emergency braking intention can be obtained, respectively.

2.2. The AEB Model of the Following Vehicle. In order to ensure that the following vehicle can avoid collision under different intentions of the driver in the front vehicle, an AEB model based on three critical braking distance calculations was established. In addition, the driving parameters and driver's intention recognition results required in the calculation of the critical braking distance were obtained via Internet of vehicles.

The critical braking distance calculation method of the proposed AEB model is shown in Figure 4. D_b is the critical braking distance of the AEB model; D_0 is a predetermined safe distance between the two vehicles, defined as 3 m; D_h is the braking distance for the entire process of the following vehicle; D_f is the braking distance for the entire process of the front vehicle. $D_{h\text{-in}}$ is the distance traveled by the following vehicle during intention recognition of the front vehicle; $D_{h\text{-tr}}$ is the distance traveled by the following vehicle during the communication delay; $D_{h\text{-bc}}$ is the distance traveled by the following vehicle when the brake pedal of the following vehicle is pressed until the braking takes effect. $D_{h\text{-br}}$ is the distance traveled during the increase of braking

deceleration of the following vehicle; $D_{h\text{-b}}$ is the distance traveled by the following vehicle during the braking of the following vehicle at a constant deceleration to the same speed v_s as the front vehicle; $D_{f\text{-bc}}$ is the distance traveled by the front vehicle when the brake pedal of the following vehicle is pressed until the brake takes effect; $D_{f\text{-br}}$ is the distance traveled during the increase of braking deceleration of the front vehicle; $D_{f\text{-b}}$ is the distance traveled by the front vehicle during the braking of the following vehicle at a constant deceleration to the same speed v_s as the front vehicle [41].

The critical braking distance of the AEB model was calculated as follows:

$$D_b = D_h + D_0 - D_f, \quad (7)$$

$$D_h = D_{h\text{-in}} + D_{h\text{-tr}} + D_{h\text{-bc}} + D_{h\text{-br}} + D_{h\text{-b}}, \quad (8)$$

$$D_f = D_{f\text{-bc}} + D_{f\text{-br}} + D_{f\text{-b}}, \quad (9)$$

$$D_{h\text{-in}} = v_h t_{\text{in}}, \quad (10)$$

$$D_{h\text{-tr}} = v_h t_{\text{tr}}, \quad (11)$$

$$D_{h\text{-bc}} = v_h t_{\text{bc}}, \quad (12)$$

$$D_{h\text{-br}} = \frac{v_h t_{\text{br}}}{2}, \quad (13)$$

$$D_{f\text{-bc}} = v_f t_{\text{bc}}, \quad (14)$$

$$D_{f\text{-br}} = \frac{v_f t_{\text{br}}}{2}, \quad (15)$$

where v_f is the speed of the front vehicle; v_h is the speed of the following vehicle; v_s is the same speed of two vehicles at the most dangerous moment; a_h is the deceleration of the following vehicle; a_f is the deceleration of the front vehicle; t_{in} is the time required to recognize the driver's intention of the front vehicle, defined as 0.4 s; t_{tr} is the transmission delay of the Internet of vehicles, and since commonly used Internet of vehicles devices based on DSRC protocol usually have a delay of a few milliseconds, while 5G network, one of the future development directions of Internet of vehicles, has a negligible delay of one millisecond, so the communication delay of vehicles in the simulation test in this paper is set to 0; t_{bc} is the time when the brake pedal of the following vehicle is pressed until the braking takes effect, defined as 0.15 s; and t_{br} is the brake deceleration increase time of the vehicle, defined as 0.45 s.

According to the driver's intention of the front vehicle and the driving conditions of the two vehicles, the parameters of $D_{h\text{-b}}$ and $D_{f\text{-b}}$ in equations (8) and (9) were changed as follows:

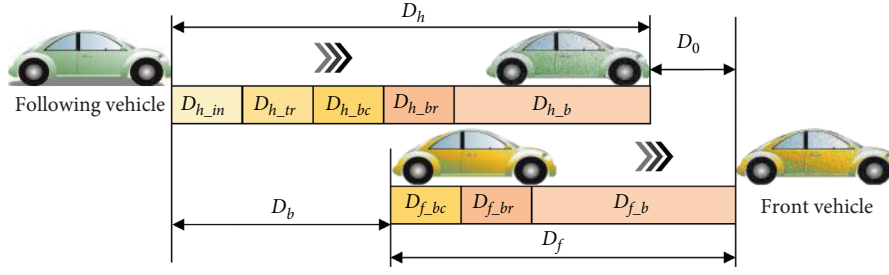


FIGURE 4: Critical braking distance calculation method.

- (i) If the two vehicles were moving at a constant speed and the following vehicle was faster than the front vehicle, the collision time occurs when the two vehicles decelerate to the same speed as the front vehicle but the following vehicle still moves faster than the front vehicle.

Then, the parameters of D_{h-b} and D_{f-b} were calculated as follows:

$$D_{f-b} = \frac{v_f(v_h - v_f)}{a_{hmax}}, \quad (16)$$

$$D_{h-b} = \frac{v_h^2 - v_f^2}{2a_{hmax}},$$

where a_{hmax} is the maximum deceleration of the following vehicle, defined as 8 m/s^2 [42].

- (ii) If the driver's intention of the front vehicle was normal braking and $v_f a_{hmax} > v_h a_f$, the collision time occurs when the two vehicles decelerate to the same speed but the following vehicle still moves faster than the front vehicle. Assume that the same vehicle speed is v_{sn} , which is defined as

$$v_{sn} = \frac{v_f a_{hmax} - v_h a_f}{a_{hmax} > a_f}. \quad (17)$$

Then, the parameters of D_{h-b} and D_{f-b} were calculated as follows:

$$D_{h-b} = \frac{v_h^2 - v_{sn}^2}{2a_{hmax}}, \quad (18)$$

$$D_{f-b} = \frac{v_f^2 - v_{sn}^2}{2a_f}.$$

If $v_f a_{hmax} \leq v_h a_f$, the collision time occurs when both vehicles slow down to stop, that is, $v_{sn} = 0$, and the distance traveled by the following vehicle is larger than that of the front vehicle.

Then, the parameters of D_{h-b} and D_{f-b} were calculated as follows:

$$D_{h-b} = \frac{v_h^2}{2a_{hmax}}, \quad (19)$$

$$D_{f-b} = \frac{v_f^2}{2a_f}.$$

- (iii) If the driver's intention of the front vehicle was emergency braking and $v_f a_{hmax} > v_h a_{fmax}$, the collision time occurs when the two vehicles decelerate to the same speed, but the following vehicle still moves faster than the front vehicle, and then the same speed of the two vehicles also is assumed as v_{se} , which is defined as

$$v_{sn} = \frac{v_f a_{hmax} - v_h a_{fmax}}{a_{hmax} > a_{fmax}}, \quad (20)$$

where a_{fmax} is the maximum deceleration of the front vehicle, defined as 6 m/s^2 .

Then, the parameters of D_{h-b} and D_{f-b} were calculated as follows:

$$D_{h-b} = \frac{v_h^2 - v_{se}^2}{2a_{hmax}}, \quad (21)$$

$$D_{f-b} = \frac{v_f^2 - v_{se}^2}{2a_{fmax}}.$$

If $v_f a_{hmax} \leq v_h a_{fmax}$, the collision time occurs when both vehicles slow down to stop, $v_{se} = 0$, and the distance traveled by the following vehicle is larger than that of the front vehicle.

Then, the parameters of D_{h-b} and D_{f-b} were calculated as follows:

$$D_{h-b} = \frac{v_h^2}{2a_{hmax}}, \quad (22)$$

$$D_{f-b} = \frac{v_f^2}{2a_{fmax}}.$$

In summary, if the relative distance d between the two vehicles is less than or equal to D_b , the proposed AEB model of the following vehicle will provide automatic braking.

3. Simulation Experiment

To verify the recognition accuracy of the driver's intention for the front vehicle and the effectiveness of the proposed AEB model, the driver's intention simulation test of the front vehicle and AEB model performance simulation test were conducted, respectively.

As shown in Figure 5, two simulation tests were carried out in Simulink and PreScan cosimulation environment, and the proposed BP-HMM model and AEB model were established in Simulink. Figure 6 shows the simulation scenario. Figure 6(a) shows the training data collection and test scenario of the proposed BP-HMM model for the front vehicle. Figure 6(b) shows the traditional AEB model performance test scenario. And Figure 6(c) shows the proposed AEB performance test scenario.

A one-way three-lane road was constructed with a length of 1 km and a width of 3.5 m for each lane in PreScan. Then, the vehicle dynamic models used 2D Simple. The following vehicle model was BMW X5, and the front vehicle was BMW Z3. The main parameters of the models are shown in Table 1. The test drivers used the G29 simulator to control the vehicle (Figures 5 and 6) in real time. Two TIS sensors in the following vehicle were used to detect the relative distance between the two vehicles. The Internet of vehicles module used the V2X sensor including a receiver and a transmitter, which was mainly used to send the driver's intention recognition results and other driving data of the front vehicle to the AEB module in following vehicle (Figure 5).

3.1. Data Collection for the Driver Intention Model. In the driver's intention simulation test, five male and five female experienced drivers were recruited as testers. Each driver used the G29 simulator to control the vehicle to drive in a straight line (Figure 6(a)). According to individual driving habits, the driver simulated uniform driving, normal braking, and emergency braking of the front vehicle within the three speed ranges of 0–30, 30–60, and 60–90 km/h and repeated the test for 20 times in each condition. Then, a total of 1,800 groups of data including brake pedal displacement, brake pedal speed, accelerator pedal displacement, accelerator pedal speed, and vehicle speed were collected. Every driver known his or her intention during the operation and can match it with the data after the test, so each group of data can represent a specific driver's intention. We take each group of data as a sample, and these 1,800 samples can constitute the dataset of the proposed BP-HMM model. Then, we divided the 1,200 samples of the dataset into training set and the remaining 600 samples into test set. In the training set and the test set, the data related to the three different driver's intentions were one-third each. Finally, the training set was used to train the BP model parameters of each driver's behavior and the HMM parameters of each driver's intention, and the test set was used to verify the recognition accuracy of the proposed BP-HMM model.

3.2. The Simulation Test for AEB. To verify the effectiveness of the proposed AEB model, we selected four traditional AEB models as comparison objects, namely, three of which

were based on safe distance, namely, Mazda [4], Honda [5], and Berkeley [6] models, and the other was the TTC [8] model based on collision to time.

The test conditions mainly refer to the two types of CCRb (Car to Car Rear braking) and CCRm (Car to Car Rear moving) for AEB testing in the European New Car Evaluation Regulations (Euro-NCAP) [43]. Since the vehicles involved in the study were all moving vehicles, CCRs (Car to Car Rear stationary) was not included in the test conditions.

According to the Euro-NCAP test standard, we changed the test conditions appropriately. The test scenarios are shown in Figures 6(b) and 6(c). Table 2 lists AEB model comparison test conditions. We shortened the 10 km/h speed interval specified in CCRm to 5 km/h and increased the maximum test speed of the following vehicle to 90 km/h, which increased the speed density of the test. Then, in the CCRb test, the brake pedal of the G29 simulator was used to provide deceleration. In the process of braking, the test driver made clear the braking intention and carried out braking operation in combination with personal driving habits. Finally, the density of test vehicle speed was also increased appropriately.

In the test, 10 experienced drivers were tested once for each driving condition, and the results of 10 tests under the same driving condition were treated as a group. When there were both collision and successful avoidance of collisions in the same group of results, the final result was calculated based on the median value of 10 tests. The results of other groups were averaged for collision speed or shortest relative distance.

4. Results

4.1. The Driver's Intention Recognition Results of the Front Vehicle. Table 3 lists the comparison of recognition accuracy of different driver intention recognition models. The single-layer BP model has a low recognition accuracy for normal braking intention (91.0%) and an average recognition rate for driver's intention (96.0%). The single-layer HMM model has the lowest recognition accuracy for uniform driving intention and normal braking intention (76.5% and 81.0%, respectively), while the average recognition rate for driver intention is only 85.17%. The accuracy rate of the BP-HMM model is above 97.0% for all three kinds of the driver's intentions, 100% for uniform driving intention, and the average recognition rate is 98%.

4.2. The AEB Simulation Test Results. Figure 7 shows the braking deceleration distribution of 10 drivers under different braking intentions in the AEB model test. Figure 7(a) shows the results of the distribution of braking deceleration of five AEB models under the driver's normal braking intention. Figure 7(b) shows the results of the distribution of braking deceleration of five AEB models under the driver's emergency braking intention. As can be seen from Figure 7, when the driver's braking intention was normal, the maximum acceleration of the front vehicle was mainly

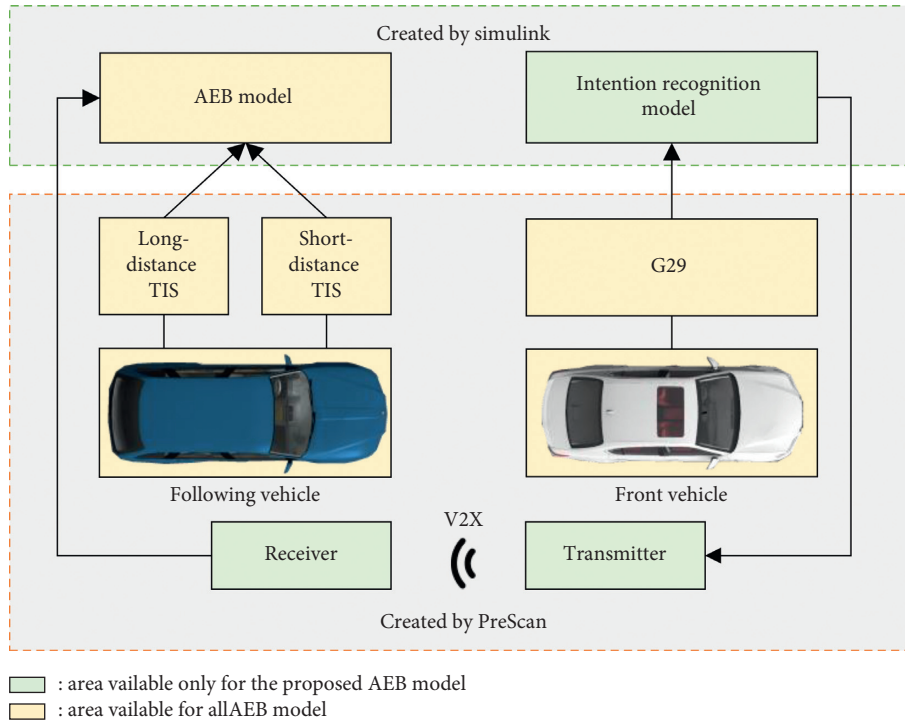


FIGURE 5: Schematic diagram of AEB model joint simulation.

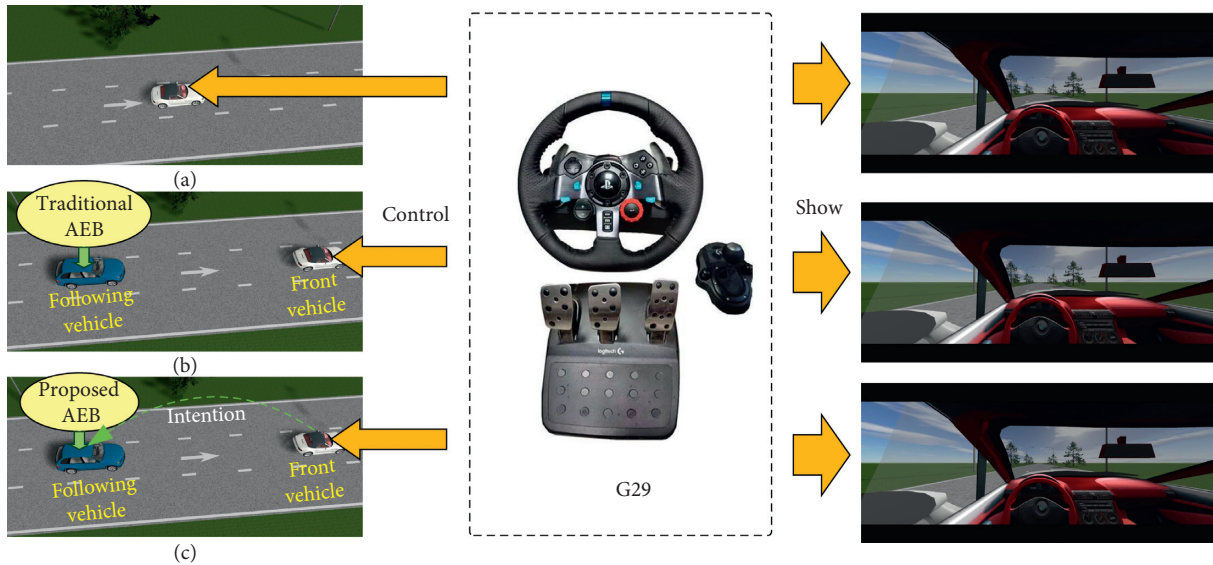


FIGURE 6: The simulation scenario: (a) the training and test scenario of the proposed BP-HMM model; (b) the traditional AEB model test scenario; (c) the proposed AEB model test scenario.

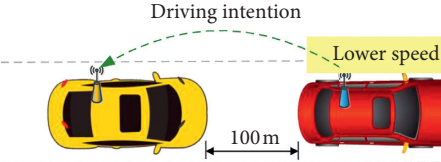
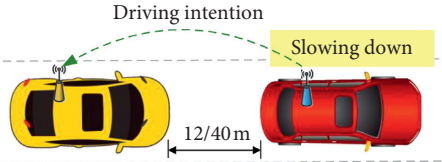
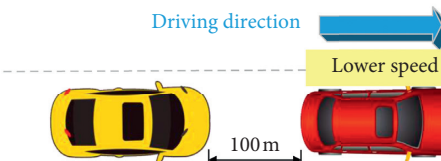
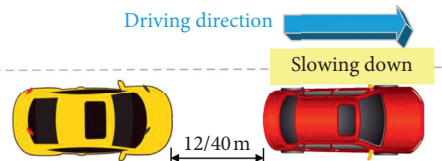
TABLE 1: Main parameters of the vehicle dynamic models.

Parameter	BMW X5	BMW Z3
Length (m)	4.790	4.040
Wide (m)	2.170	1.960
High (m)	1.720	1.230
Wheelbase (m)	2.820	2.446
Mass (kg)	2220	1435
Maximum braking pressure (MPa)	15	15
Maximum acceleration (m/s^2)	3	3
Maximum deceleration (m/s^2)	8	6

concentrated between -1.5 and $-3.0 m/s^2$. When the driver's braking intention was emergency, the maximum deceleration of the front vehicle was mainly concentrated between -5.0 and $-6.0 m/s^2$.

Figures 8 and 9, respectively, show the comparison diagram of the shortest relative distance between two vehicles in the CCRm and CCRb tests of the five AEB models. As shown in Figure 8, in the CCRm test of the Mazda model, as the vehicle speed increased, the shortest relative distance d_{end} of the two vehicles also increased, with a range between

TABLE 2: AEB model comparison test conditions.

Scenario	Car to Car Rear moving (CCRM)		Car to Car Rear braking (CCRB)	
Proposed AEB				
Traditional AEB				
Object	Following vehicle	Front vehicle	Both vehicles	Front vehicle
Initial parameter setting	(1) 30 km/h		(1) 10 km/h	
	(2) 35 km/h		(2) 20 km/h	
	(3) 40 km/h		(3) 30 km/h	
	(4) 45 km/h		(4) 40 km/h	
	(5) 50 km/h		(5) 50 km/h	(1) Testers braking with NBI intention
	(6) 55 km/h		(6) 60 km/h	(2) Testers braking with EBI
	(7) 60 km/h	20 km/h (UDI)	(7) 70 km/h	
	(8) 65 km/h		(8) 80 km/h	
	(9) 70 km/h		(9) 90 km/h	
	(10) 75 km/h			
	(11) 80 km/h			
	(12) 85 km/h			
	(13) 90 km/h			

UDI: uniform driving intention; NBI: normal braking intention; EBI: emergency braking intention.

TABLE 3: Comparison of recognition accuracy of different driver's intention recognition models.

Model	Driver's intention	Uniform driving	Normal braking	Emergency braking	Accuracy (%)	Average accuracy (%)
BP	Uniform driving	198	2	0	99.0	96.000
	Normal braking	15	182	3	91.0	
	Emergency braking	0	4	196	98.0	
HMM	Uniform driving	153	40	7	76.5	85.167
	Normal braking	38	162	0	81.0	
	Emergency braking	0	4	196	98.0	
BP-HMM	Uniform driving	200	0	0	100.0	98.000
	Normal braking	3	194	3	97.0	
	Emergency braking	0	6	194	97.0	

4.48 m and 17.61 m. The performance of Honda and Berkeley models was similar, and the range of d_{end} was mainly between 4 m and 10 m. Although the TTC model managed to avoid collision in the speed range of 30–65 km/h, it failed to avoid rear-end collision in the range of 70–90 km/h. For the proposed AEB model, the d_{end} was stable between 1.5 m and 2.7 m.

As shown in Figure 9(a), The Honda, Berkeley, and TTC models were unable to avoid a collision at a speed range of 60–90 km/h when two vehicles were trailing at a distance of 40 m and the driver in front vehicle was making an emergency stop. However, Mazda and the proposed AEB models were able to successfully avoid collisions at all

speed ranges of the test. As shown in Figure 9(b), when the test condition was changed to the front vehicle with normal braking intention, only the TTC model had a collision in the speed range of 80–90 km/h. When the distance between the two vehicles was 12 m and the front vehicle was on emergency braking, as shown in Figure 9(c), the Mazda model and the proposed AEB model still successfully avoided collision. In addition, when the driver of the front vehicle wanted to change from emergency braking to normal braking, as shown in Figure 9(d), all five AEB models avoided collisions. It is worth noting that the d_{end} of the proposed AEB model was stable between 2.63 m and 5.28 m during the CCRB test.

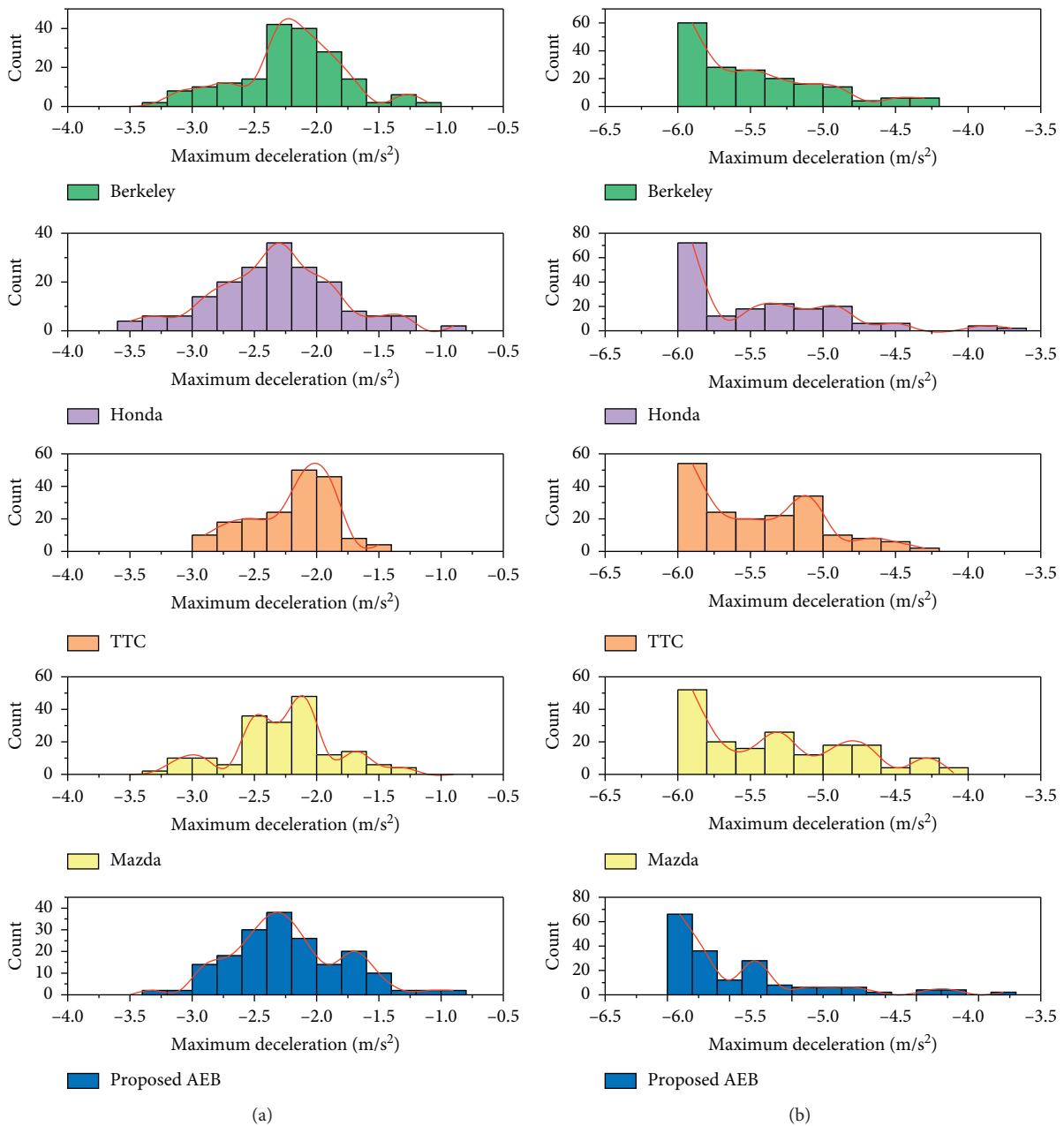


FIGURE 7: Braking deceleration distribution of drivers under different braking intentions: (a) normal braking intention; (b) emergency braking intention.

Figure 10 shows a comparison of the number of successful collisions avoided by each model in the CCRb test scenario. When the collision occurred during the test, the initial speeds of both vehicles were relatively high, between 60 and 90 km/h. The Mazda model and the proposed AEB model avoided collision in all speed ranges of the test conditions, and the TTC model had the least number of successful collision avoidance among the five models.

In the CCRb test, the vehicle speed distribution in case of collision of the TTC, Berkeley, and Honda models are shown in Figure 11. All three models collided when the initial vehicle speed was higher than 60 km/h and the driver had emergency braking intention (EBI). It is worth noting that the TTC

model failed to avoid collision when the initial speed was higher than 80 km/h, the distance between the vehicles was 40 m, and the driver had normal braking intention (NBI).

5. Discussion

We can see from Table 2 that the single-layer HMM model had the worst effect on the recognition of uniform driving intention and normal braking intention. Although the HMM model had strong mapping ability for data with temporal relation, it was not suitable for the classification of large data volume. Due to the large dimension and length of the input single sample data and the large number of samples

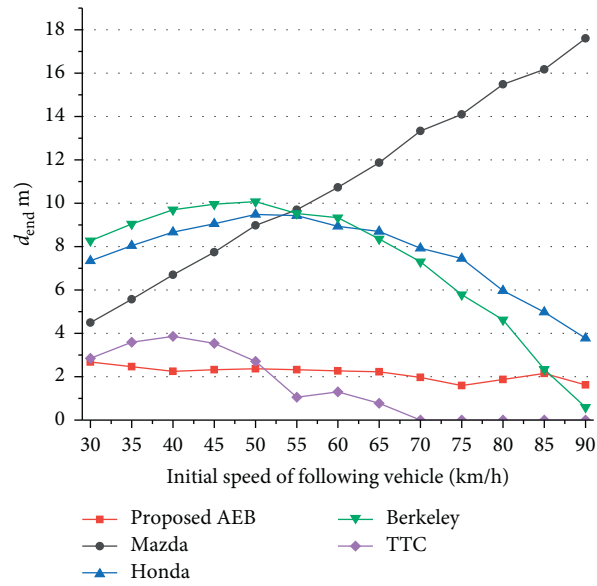


FIGURE 8: The shortest relative distance between two vehicles in the CCRm scenario test.

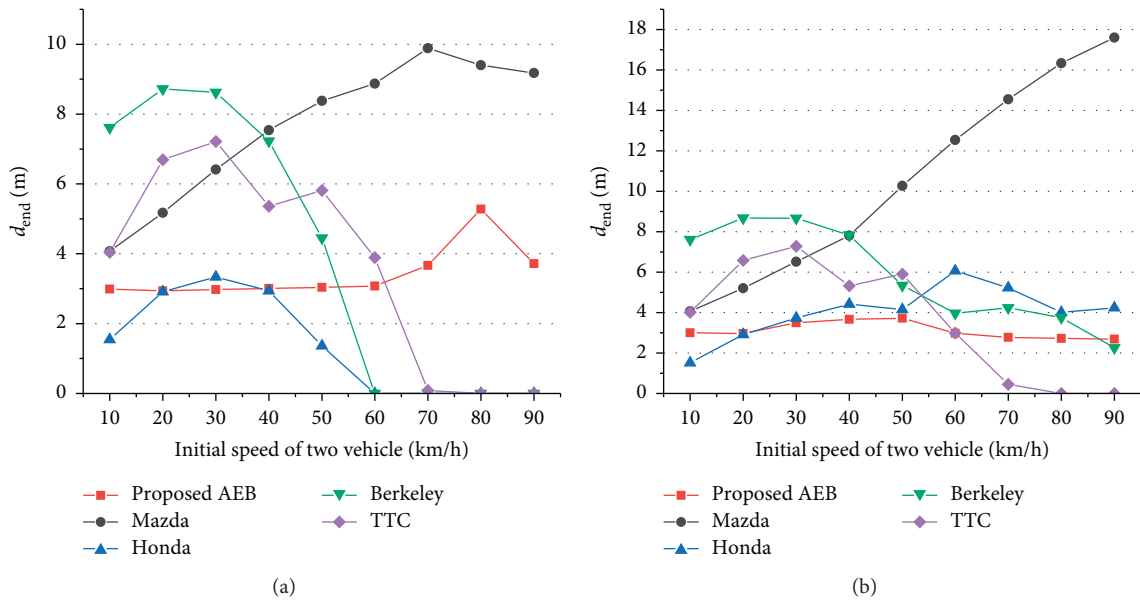


FIGURE 9: Continued.

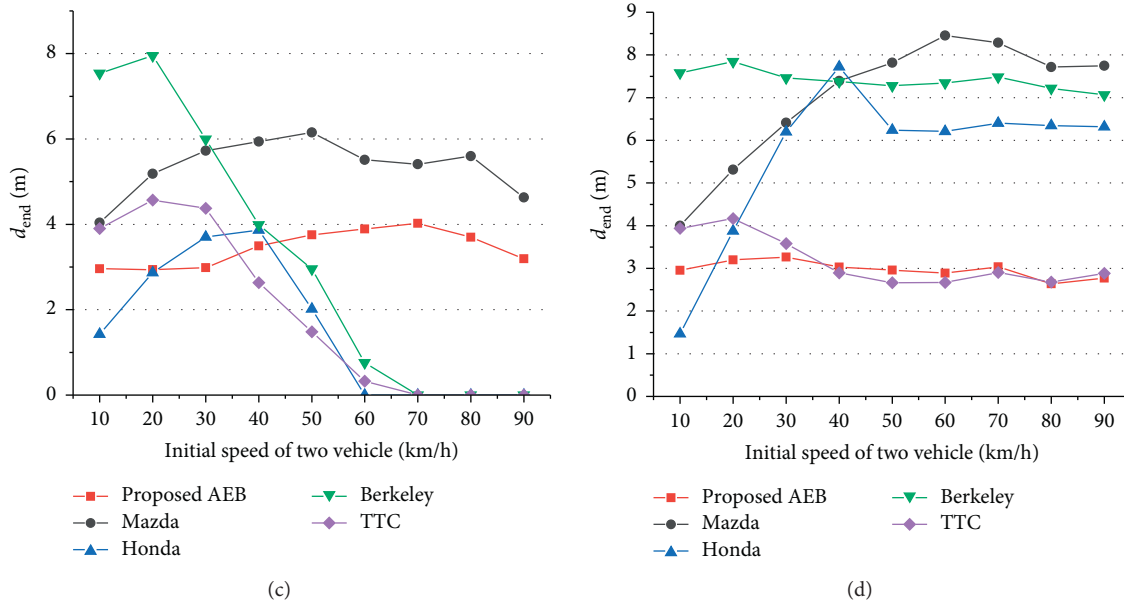


FIGURE 9: The shortest relative distance between two vehicles in the CCRb scenario test: (a) CCRb-40 m emergency braking intention; (b) CCRb-40 m normal braking intention; (c) CCRb-12 m emergency braking intention; (d) CCRb-12 m normal braking intention.

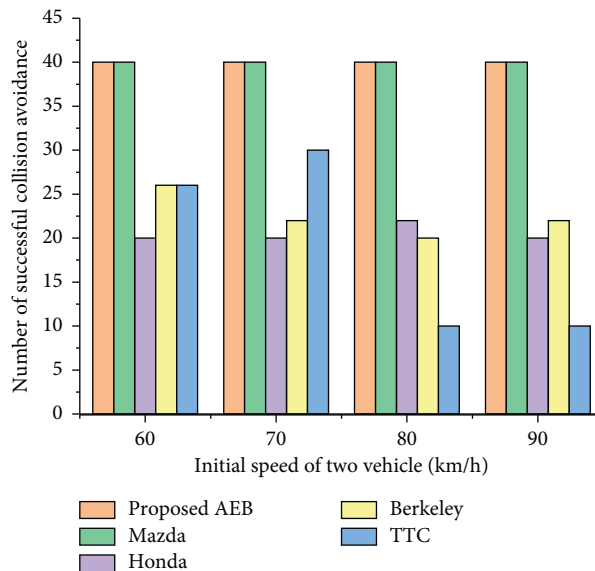


FIGURE 10: Comparison of the number of successful avoidance collisions between the models.

trained at the same time, the classification effect was not very well. The single-layer BP neural network can be used for the classification of the large amount of data. Although the overall recognition effect of intention recognition was good, it was easy to misidentify the normal braking intention as the other two intentions. However, the BP-HMM model had the best recognition effect, with an accuracy rate of 100% for the uniform driving intention and an average recognition rate of 98% for each intention. The recognition results show that the combination of the BP neural network and HMM can improve the classification accuracy of large data volume.

During the five AEB model tests (Figure 6), although the same driver or different drivers had different operations each

time, when drivers had the same braking intention, the braking deceleration distribution trend of the front vehicle was basically the same. Therefore, under the same braking condition, the influence of drivers at different times on different model test results can be ignored.

Although the Mazda model was able to avoid collision in both CCRm and CCRb tests (Figures 7 and 8), the braking strategy was too conservative, especially at high speeds, and was easy to cause unnecessary interference to the driver. The braking strategies of the Honda and Berkeley models were more aggressive than the Mazda model, and the performance of the two models in CCRm tests was similar. In the CCRb test, the two models performed better

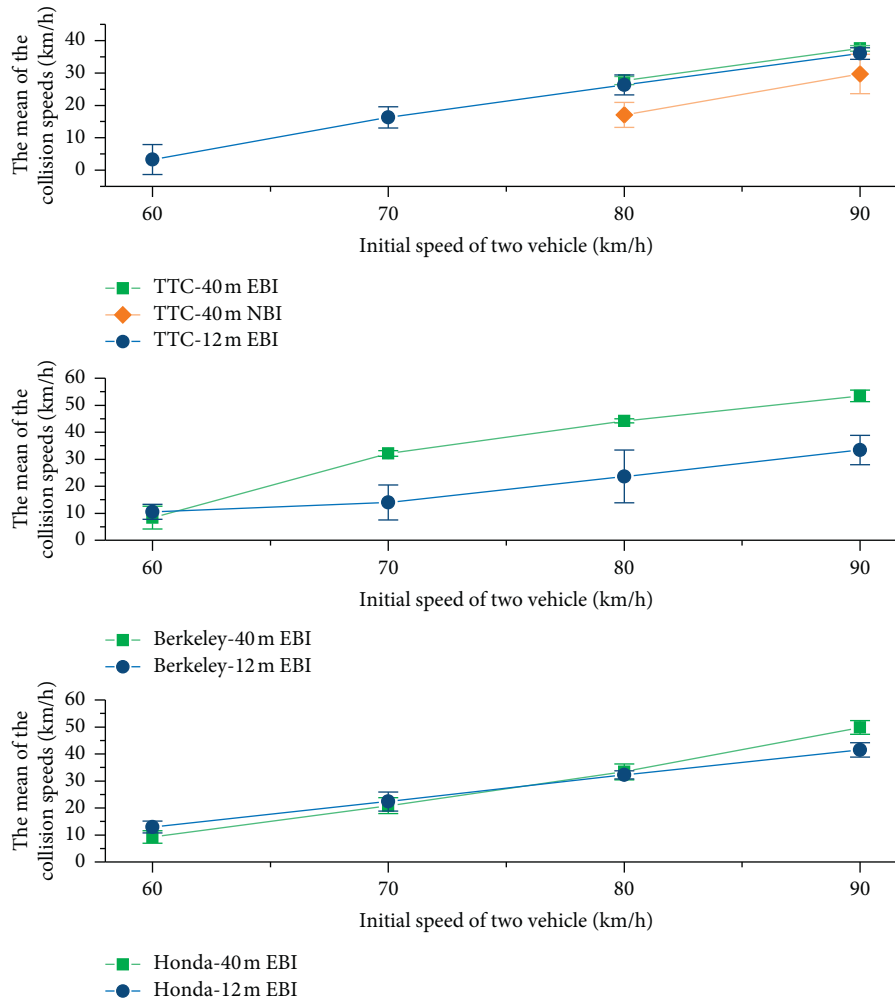


FIGURE 11: The vehicle speed distribution of each model in the event of collision.

when the driver’s intention of the front vehicle was normal braking intention. However, in the case of high-speed driving and emergency braking intention of the front vehicle, the collision cannot be avoided successfully, and the braking strategy is more inclined to the safety of low speed driving. In these five models, the performance of the TTC model was relatively poor; also, in CCRm tests, collision happened. Although collision avoidance can be achieved by adjusting the braking threshold, it will lead to the model being more conservative at low speed. However, the proposed AEB model can not only successfully avoid collisions under all conditions but also keep the shortest relative distance between the two vehicles at about 3 m during braking. Unlike the Mazda model, it is not conservative and can avoid high-speed collision accidents, which improves the collision avoidance performance and acceptability of the AEB system.

All models performed well at low speeds, and collisions mainly occurred when the following vehicle was traveling at high speed and the front vehicle had braking intention. As shown in Figures 9 and 10, in the CCRb test, collisions occurred in the Honda, Berkeley, and TTC model tests when the speed was faster than 60 km/h, especially in the

emergency braking of the front vehicle. Since the AEB model needs a period of time to detect risks, during this period, with the increase of initial test speed or the increase of braking strength of the front vehicle, the distance between the two vehicles will decrease relatively, resulting in an increased risk of collision. The TTC model presented the dangerous situations under normal braking of the front vehicle, which cannot well reflect the collision risk when the vehicle suddenly brakes (especially in a small relative distance). However, when the relative speed between the two vehicles was high, the collision avoidance performance of TTC will be affected. Although the above model failed to avoid collision under some driving conditions, it still reduced the collision speed and the loss caused by the collision.

In summary, the parameters of the traditional model are fixed values, and the ability to adjust according to the driving intention or the change of the state of the front vehicle is insufficient, which is only applicable to some driving conditions. However, the proposed model can adjust the braking strategy according to the driving intention of the front vehicle, with stronger adaptive ability.

6. Conclusion

In this paper, we proposed an AEB model based on the driver's intention recognition of the front vehicle via Internet of vehicles. A BP-HMM model was proposed to recognize the driver's intention of the front vehicle. The recognized driver's intention was transmitted via Internet of vehicles; then, an AEB model for the following vehicle was proposed to calculate the critical braking distance under different driving conditions to avoid rear-end collision. In the driver's intention recognition simulation test, the proposed BP-HMM model exhibited better result on the driver's intention recognition than the previous single-layer BP and single-layer HMM models. The AEB simulation test results demonstrated that compared with the traditional AEB model, the proposed AEB model provided more effective braking to avoid rear-end collision under different test conditions and made the AEB system safer and more comfortable without triggering braking too early or too late.

Data Availability

The data used to support the findings of this study are available from the corresponding author upon request.

Conflicts of Interest

The authors declare that they have no conflicts of interest.

Acknowledgments

The first author would like to acknowledge Prof. Lang Wei at Chang'an University for providing suggestions and helpful discussions. This work was supported in part by the National Natural Science Foundation (grant no. 51278062), the Shaanxi Province Science Foundation for Youths (grant no. 2017JQ6045), and the Fundamental Research Funds for the Central Universities (grant no. 300102229112).

References

- [1] X. Xiang, W. Qin, and B. Xiang, "Research on a DSRC-based rear-end collision warning model," *IEEE Transactions on Intelligent Transportation Systems*, vol. 15, no. 3, pp. 1054–1065, 2014.
- [2] N. Arbabzadeh, M. Jafari, M. Jalayer, S. Jiang, and M. Kharbeche, "A hybrid approach for identifying factors affecting driver reaction time using naturalistic driving data," *Transportation Research Part C: Emerging Technologies*, vol. 100, pp. 107–124, 2019.
- [3] B. Fildes, M. Keall, N. Bos et al., "Effectiveness of low speed autonomous emergency braking in real-world rear-end crashes," *Accident Analysis & Prevention*, vol. 81, pp. 24–29, 2015.
- [4] J. B. Cicchino, "Effectiveness of forward collision warning and autonomous emergency braking systems in reducing front-to-rear crash rates," *Accident Analysis & Prevention*, vol. 99, no. A, pp. 142–152, 2017.
- [5] Y. Fujita, K. Akuzawa, and M. Sato, "Radar brake system," *JSAE Review*, vol. 16, no. 2, p. 219, 1995.
- [6] P. Seiler, B. Song, and J. K. Hedrick, "Development of a collision avoidance system," in *Proceedings of the 1998 SAE International Congress and Exposition*, Detroit, MI, USA, February 1998.
- [7] H. Yoshida, S. Awano, M. Nagai, and T. Kamada, "Target following brake control for collision avoidance assist of active interface vehicle," in *Proceedings of the 2006 SICE-ICASE International Joint Conference*, pp. 4436–4439, Busan, Korea, October 2006.
- [8] K. D. Kusano and H. Gabler, "Method for estimating time to collision at braking in real-world, lead vehicle stopped rear-end crashes for use in pre-crash system design," *SAE International Journal of Passenger Cars—Mechanical Systems*, vol. 4, no. 1, pp. 435–443, 2011.
- [9] K. Lee and H. Peng, "Evaluation of automotive forward collision warning and collision avoidance algorithms," *Vehicle System Dynamics*, vol. 43, no. 10, pp. 735–751, 2005.
- [10] D. Katare and M. El-Sharkawy, "Embedded system enabled vehicle collision detection: an ANN classifier," in *Proceedings of the 2019 IEEE 9th Annual Computing and Communication Workshop and Conference (CCWC)*, pp. 284–289, Las Vegas, NV, USA, January 2019.
- [11] Y. L. Chen, K. Y. Shen, and S. C. Wang, "Forward collision warning system considering both time-to-collision and safety braking distance," in *Proceedings of the 2013 IEEE 8th Conference on Industrial Electronics and Applications (ICIEA)*, pp. 972–977, Melbourne, Australia, June 2013.
- [12] N. Kaempchen, B. Schiele, and K. Dietmayer, "Situation assessment of an autonomous emergency brake for arbitrary vehicle-to-vehicle collision scenarios," *IEEE Transactions on Intelligent Transportation Systems*, vol. 10, no. 4, pp. 678–687, 2009.
- [13] X. F. Pei, Z. Q. Qi, B. F. Wang et al., "Vehicle frontal collision warning/avoidance strategy," *Journal of Jilin University (Engineering and Technology Edition)*, vol. 44, no. 3, pp. 599–604, 2014.
- [14] I. C. Han, B. C. Luan, and F. C. Hsieh, "Development of autonomous emergency braking control system based on road friction," in *Proceedings of the 2014 IEEE International Conference on Automation Science and Engineering (CASE)*, pp. 933–937, Taipei, Taiwan, August 2014.
- [15] T. Kim, J. Lee, and K. Yi, "Enhanced maximum tire-road friction coefficient estimation based advanced emergency braking algorithm," in *Proceedings of the 2015 IEEE Intelligent Vehicles Symposium (IV)*, pp. 883–888, Seoul, South Korea, June 2015.
- [16] Y. Hwang and S. B. Choi, "Adaptive collision avoidance using road friction information," *IEEE Transactions on Intelligent Transportation Systems*, vol. 20, no. 1, pp. 348–361, 2019.
- [17] H. Kim, K. Shin, I. Chang, and K. Huh, "Autonomous emergency braking considering road slope and friction coefficient," *International Journal of Automotive Technology*, vol. 19, no. 6, pp. 1013–1022, 2018.
- [18] G. Li, Y. Wang, F. Zhu et al., "Drivers' visual scanning behavior at signalized and unsignalized intersections: a naturalistic driving study in China," *Journal of Safety Research*, vol. 71, pp. 219–229, 2019.
- [19] G. F. Li, W. J. Lai, X. X. Sui et al., "Influence of traffic congestion on driver behavior in post-congestion driving," *Accident Analysis & Prevention*, vol. 141, p. 105508, 2020.
- [20] X. Xiong, M. Wang, Y. Cai, L. Chen, H. Farah, and M. Hagenzieker, "A forward collision avoidance algorithm based on driver braking behavior," *Accident Analysis & Prevention*, vol. 129, pp. 30–43, 2019.

- [21] J. Duan, R. Li, L. Hou et al., "Driver braking behavior analysis to improve autonomous emergency braking systems in typical Chinese vehicle-bicycle conflicts," *Accident Analysis & Prevention*, vol. 108, pp. 74–82, 2017.
- [22] T. Wada, S. i. Doi, N. Tsuru, K. Isaji, and H. Kaneko, "Characterization of expert drivers' last-second braking and its application to a collision avoidance system," *IEEE Transactions on Intelligent Transportation Systems*, vol. 11, no. 2, pp. 413–422, 2010.
- [23] J. Wang, C. Yu, S. E. Li, and L. Wang, "A forward collision warning algorithm with adaptation to driver behaviors," *IEEE Transactions on Intelligent Transportation Systems*, vol. 17, no. 4, pp. 1157–1167, 2016.
- [24] F. Bella and R. Russo, "A collision warning system for rear-end collision: a driving simulator study," *Procedia—Social and Behavioral Sciences*, vol. 20, pp. 676–686, 2011.
- [25] S. H. Lee, S. Lee, and M. H. Kim, "Development of a driving behavior-based collision warning system using a neural network," *International Journal of Automotive Technology*, vol. 19, no. 5, pp. 837–844, 2018.
- [26] X. Wang, M. Chen, M. Zhu, and P. Tremont, "Development of a kinematic-based forward collision warning algorithm using an advanced driving simulator," *IEEE Transactions on Intelligent Transportation Systems*, vol. 17, no. 9, pp. 2583–2591, 2016.
- [27] W. Yuan, Z. Li, and C. Wang, "Lane-change prediction method for adaptive cruise control system with hidden Markov model," *Advances in Mechanical Engineering*, vol. 10, no. 9, pp. 168781401880293–168781401880299, 2018.
- [28] X. Geng, H. Liang, B. Yu, P. Zhao, L. He, and R. Huang, "A scenario-adaptive driving behavior prediction approach to urban autonomous driving," *Applied Sciences*, vol. 7, no. 4, p. 426, 2017.
- [29] Y. P. Hu, W. Zhan, and M. Tomizuka, "Probabilistic prediction of vehicle semantic intention and motion," in *Proceedings of the 2018 IEEE Intelligent Vehicles Symposium (IV)*, pp. 307–313, Changshu, Suzhou, China, June 2018.
- [30] K. Jo, M. Lee, J. Kim, and M. Sunwoo, "Tracking and behavior reasoning of moving vehicles based on roadway geometry constraints," *IEEE Transactions on Intelligent Transportation Systems*, vol. 18, no. 2, pp. 460–476, 2017.
- [31] J. Choi, V. Va, N. Gonzalez-Prelcic, R. Daniels, C. R. Bhat, and R. W. Heath, "Millimeter-wave vehicular communication to support massive automotive sensing," *IEEE Communications Magazine*, vol. 54, no. 12, pp. 160–167, 2016.
- [32] X. Zhao, S. Jing, F. Hui, R. Liu, and A. J. Khattak, "DSRC-based rear-end collision warning system - an error-component safety distance model and field test," *Transportation Research Part C: Emerging Technologies*, vol. 107, pp. 92–104, 2019.
- [33] V. Milanés, J. Villagrà, J. Godoy, J. Simo, J. Perez, and E. Onieva, "An intelligent V2I-based traffic management system," *IEEE Transactions on Intelligent Transportation Systems*, vol. 13, no. 1, pp. 49–58, 2012.
- [34] C. Wu, L. Peng, Z. Huang, M. Zhong, and D. Chu, "A method of vehicle motion prediction and collision risk assessment with a simulated vehicular cyber physical system," *Transportation Research Part C: Emerging Technologies*, vol. 47, no. 2, pp. 179–191, 2014.
- [35] L. Thomas, S. T. Panicker, and T. Tony, "DSRC based collision warning for vehicles at intersections," in *Proceedings of the 2016 3rd International Conference on Advanced Computing and Communication Systems (ICACCS)*, Coimbatore, India, January 2016.
- [36] Y. Liu, Z.-L. Wang, and B.-G. Cai, "Investigation of a DSRC-based end of queue collision warning system by considering real freeway data," *IET Intelligent Transport Systems*, vol. 13, no. 1, pp. 108–114, 2019.
- [37] D. Tian, Y. Yuan, J. Wang, and H. Xia, "Collision avoidance on winding roads using dedicated short-range communication," *Transport*, vol. 33, no. 2, pp. 461–469, 2017.
- [38] S. Al-Sultan, A. H. Al-Bayatti, and H. Zedan, "Context-aware driver behavior detection system in intelligent transportation systems," *IEEE Transactions on Vehicular Technology*, vol. 62, no. 9, pp. 4264–4275, 2013.
- [39] J. Hu, L. Xu, X. He, and W. Meng, "Abnormal driving detection based on normalized driving behavior," *IEEE Transactions on Vehicular Technology*, vol. 66, no. 8, pp. 6645–6652, 2017.
- [40] L. R. Welch, "Hidden Markov models and the Baum-Welch algorithm," *IEEE ITS Newsletter*, vol. 53, pp. 194–211, 2003.
- [41] D. F. Llorca, S. Sánchez, M. Ocaña, and M. A. Sotelo, "Vision-based traffic data collection sensor for automotive applications," *Sensors*, vol. 10, no. 1, pp. 860–875, 2010.
- [42] T. Chen, K. Liu, Z. Wang, G. Deng, and B. Chen, "Vehicle forward collision warning algorithm based on road friction," *Transportation Research Part D: Transport and Environment*, vol. 66, pp. 49–57, 2019.
- [43] EURO NCAP, "Test protocol-AEB systems version 1.1," 2015, <https://www.euroncap.com/en/for-engineers/protocols/safety-assist>.